

Supplementary Information

New insights into Late Pleistocene cave hyena chronology and population history – the case of Perspektywiczna Cave, Poland

Maciej T. Krajcarz¹, Mateusz Baca², Chris Baumann^{3,4}, Hervé Bocherens^{3,5}, Tomasz Goslar⁶, Danijela Popović², Magdalena Sudoł-Procyk⁸, Magdalena Krajcarz^{*3,8}

¹ Institute of Geological Sciences, Polish Academy of Sciences, Twarda 51/55, 00-818, Warsaw, Poland, e-mail: mkrajcarz@twarda.pan.pl

² Centre of New Technologies, University of Warsaw, S. Banacha 2c, 02-097, Warsaw, Poland, e-mails: m.baca@cent.uw.edu.pl, d.popovic@cent.uw.edu.pl

³ Department of Geosciences, Biogeology, University of Tübingen, Hölderlinstrasse 12, 72074, Tübingen, Germany, e-mails: magkrajcarz@umk.pl; chris.baumann@uni-tuebingen.de; herve.bocherens@uni-tuebingen.de

⁴ Department of Geosciences and Geography, University of Helsinki, Finland

⁵ Senckenberg Centre for Human Evolution and Palaeoenvironment (S-HEP), Hölderlinstrasse 12, 72074, Tübingen, Germany

⁶ Faculty of Geographical and Geological Sciences, Adam Mickiewicz University, B. Krygowskiego 10, 61-680 Poznań, Poland, mail: goslar@radiocarbon.pl

⁸ Institute of Archaeology, Nicolaus Copernicus University in Toruń, Szosa Bydgoska 44/48, 87-100, Toruń, Poland, e-mails: sudol@umk.pl; magkrajcarz@umk.pl

*corresponding author. Email: magkrajcarz@umk.pl

Contents

| | |
|-----------------------------------|---|
| Figure S1. | 2 |
| Figure S2. | 3 |
| Figure S3. | 4 |
| Phylogenetic reconstruction | 5 |
| OxCal codes | 7 |

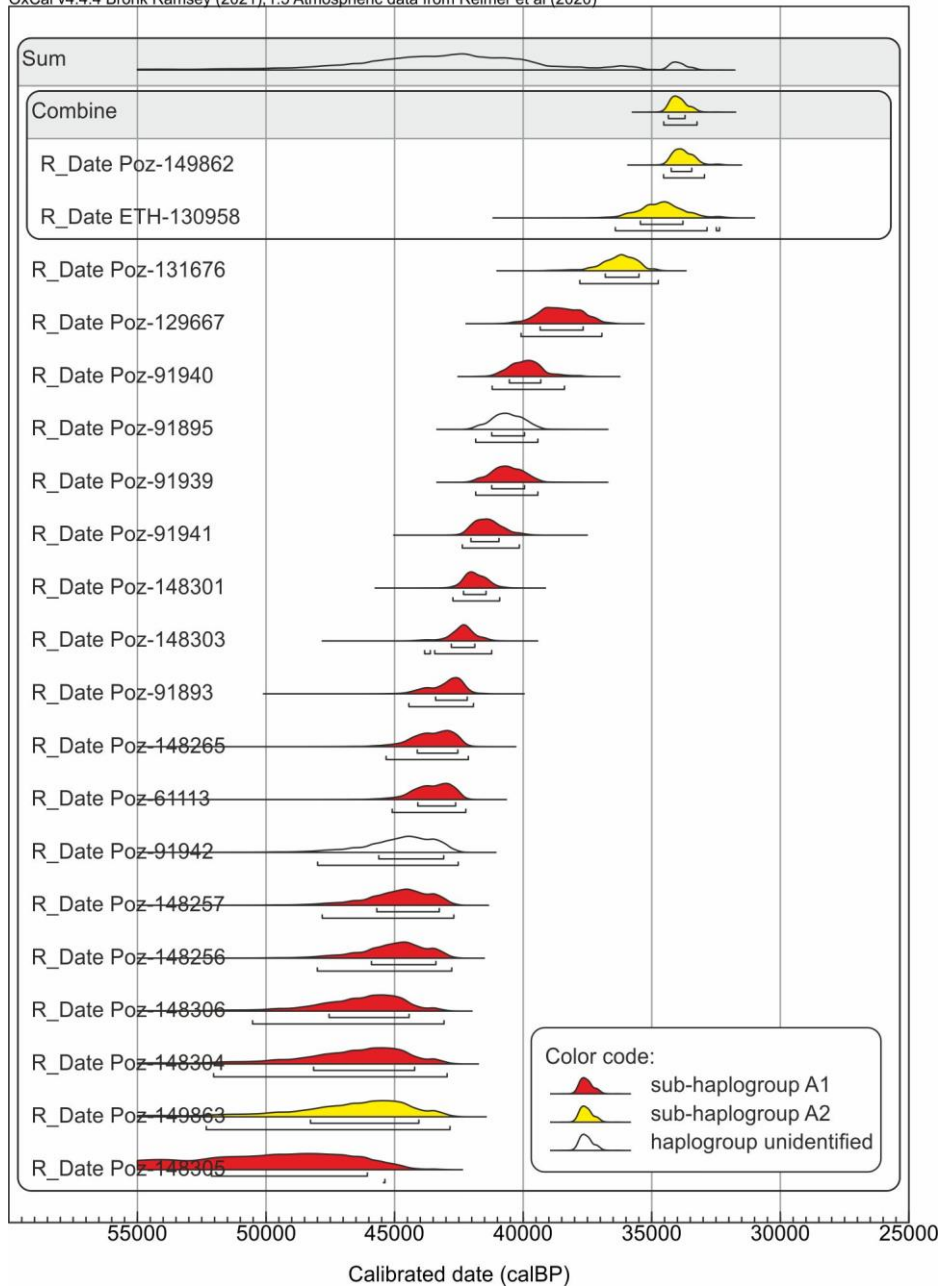


Figure S1. Distribution of calibrated radiocarbon dates of cave hyena remains from Perspektywiczna Cave. Two segments below each likelihood plot represent the posterior probability ranges for 68.3% probability (upper ones) and 95.4% probability (lower ones).



Figure S2. Maximum clade credibility tree generated using modern and ancient hyaena mitogenomes in BEAST 1.10.4. Numbers at nodes are *posterior probabilities*, grey bars represent 95% highest posterior density intervals of node ages.



Figure S3. Specimen CRO001 from Perspektywiczna Cave, the Upper Chamber, layer C1 (collection ID: Udórz IVc W-199, stored in the Institute of Archaeology, Nicolaus Copernicus University, Toruń, Poland). Adult right ulna, a lateral view; distal part of a shaft and distal epiphysis are missing (gnawed off).

Phylogenetic reconstruction

To confirm taxonomic assignment and estimate the phylogenetic position of hyaena remains from Perspektywiczna cave we gathered a dataset consisting of 44 modern and ancient hyaena mitogenomes. Twenty-five sequences were obtained previously and 19 were generated in this study. We used mitogenomes of *Parahyaena brunnea* (MF593938) and *Hyaena hyaena* (JF894376.1) as outgroups. Sequences were aligned in MAFFT v7.407 (Katoh and Standley, 2013) resulting in an alignment with 17290 positions. The most appropriate partitioning scheme and DNA substitution models were selected using PartitionFinder 2 (Lanfear et al., 2016). We set PartitionFinder 2 to choose from the DNA substitution models available in BEAST software and to use BIC to discriminate between models (Table S1).

Table S1. Best partitioning scheme of mitochondrial DNA and DNA substitution models identified by PartitionFinder2.

| Subset | Best Model | # sites | Partitions |
|--------|------------|---------|--|
| 1 | HKY+I+G+X | 1924 | noncoding |
| 2 | TRN+I+X | 5836 | tRNAs, rRNAs, ND4_cp3, ND5_cp1, ATP6_cp1, ND2_cp1, ND6_cp3 |
| 3 | K80+I | 1918 | COX1_cp1, COX2_cp1, ND4L_cp1, COX3_cp3, ND3_cp1, cyb_cp1, ND1_cp1 |
| 4 | HKY+I+X | 3556 | COX1_cp2, ND2_cp2, COX3_cp1, ND4_cp1, ATP6_cp2, ND4L_cp2, ND5_cp2, cyb_cp2, ND3_cp2, COX2_cp2, ND1_cp2 |
| 5 | HKY+X | 1160 | ND2_cp3, ND1_cp3, ND3_cp3, cyb_cp3 |
| 6 | TRN+G+X | 2617 | COX1_cp3, COX2_cp3, ND6_cp2, ND5_cp3, ND4_cp2, COX3_cp2, ND4L_cp3, ATP6_cp3, ATP8_cp3 |
| 7 | TRN+X | 279 | ND6_cp1, ATP8_cp1, ATP8_cp2 |

The phylogenetic reconstruction was performed in BEAST 1.10.4 (Suchard et al., 2018). We set the strict clock for all analyses. For the radiocarbon dated specimens we used medians of calibrated dates as tip dates. In the case of four specimens without radiocarbon dates we used medians of previously estimated ages as tip dates. In the case of two specimens from Perspektywiczna cave which were not radiocarbon dated we estimated their ages using the tip dating approach (Shapiro et al., 2011). We set the gamma priors (shape=2; scale=50000) on the ages of these two specimens. We used the divergence time of *Crocuta* and *Parahyaena/Hyaena* to additionally calibrate the phylogeny. We set a normal prior (mean=9.5 Ma; sd=0.3 Ma) on the age of this divergence following Hu et al. (2021) and used CTMC reference rate prior on substitution rate. To test which of three tree priors (constant population size, Skygrid or skyride) fits best to our dataset we estimated log marginal likelihoods (MLE) of respective models using the generalised stepping-stone (GSS) sampling approach (Baele et al., 2016). We run each analysis for 100 million generations with trees sampled every 10 thousand generations. The MLE calculation consisted of 100 steps, each run for one million iterations. All three analyses were run in duplicates, convergence and stationarity were inspected in Tracer 1.7 (Rambaut et

al., 2018). The skyride tree prior was noticeably inferior comparing to the two others ($2\text{LnBF} = -303.5$ in both comparisons), while constant pop. size and Skyride tree priors were not significantly different ($2\text{LnBF} = -1.25$), so we used simpler constant population size tree prior (Table S2). The two replicates of the selected analysis were combined using *logcombiner* with first 10 million generations removed from each replicate as burn-in. The trees were summarized, and *Maximum Clade Credibility* tree was generated using *treeannotator*.

Table S2. Results of tree prior testing using GSS

| Model | Replicate 1 | Replicate 2 | mean LnL |
|-------------------------------|-------------|-------------|-----------------|
| constant pop. size tree prior | -40676,9 | -40677,4 | -40677,1 |
| Skygrid tree prior | -40676,3 | -40679,2 | -40677,8 |
| skyride tree prior | -40828,8 | -40828,9 | -40828,9 |

- Baele, G., Lemey, P., Suchard, M.A., 2016. Genealogical Working Distributions for Bayesian Model Testing with Phylogenetic Uncertainty. *Syst Biol* 65, 250–264. <https://doi.org/10.1093/sysbio/syv083>
- Hu, J., Westbury, M. V., Yuan, J., Zhang, Z., Chen, S., Xiao, B., Hou, X., Ji, H., Lai, X., Hofreiter, M., Sheng, G., 2021. Ancient mitochondrial genomes from Chinese cave hyenas provide insights into the evolutionary history of the genus *Crocuta*. *Proceedings of the Royal Society B: Biological Sciences* 288. <https://doi.org/10.1098/rspb.2020.2934>
- Katoh, K., Standley, D.M., 2013. MAFFT multiple sequence alignment software version 7: Improvements in performance and usability. *Mol Biol Evol* 30, 772–780. <https://doi.org/10.1093/molbev/mst010>
- Lanfear, R., Frandsen, P.B., Wright, A.M., Senfeld, T., Calcott, B., 2016. PartitionFinder 2: New methods for selecting partitioned models of evolution for molecular and morphological phylogenetic analyses. *Mol Biol Evol* 34, msw260. <https://doi.org/10.1093/molbev/msw260>
- Rambaut, A., Drummond, A.J., Xie, D., Baele, G., Suchard, M.A., 2018. Posterior summarization in Bayesian phylogenetics using Tracer 1.7. *Syst Biol* 67, 901–904. <https://doi.org/10.1093/sysbio/syy032>
- Shapiro, B., Ho, S.Y.W., Drummond, A.J., Suchard, M.A., Pybus, O.G., Rambaut, A., 2011. A bayesian phylogenetic method to estimate unknown sequence ages. *Mol Biol Evol* 28, 879–887. <https://doi.org/10.1093/molbev/msq262>
- Suchard, M.A., Lemey, P., Baele, G., Ayres, D.L., Drummond, A.J., Rambaut, A., 2018. Bayesian phylogenetic and phylodynamic data integration using BEAST 1.10. *Virus Evol* 4, 1–5. <https://doi.org/10.1093/ve/vey016>

OxCal codes

OxCal code for sum of distributions of all Perspektywiczna Cave hyenas

```
Sum("PC hyenas")
{
  Combine (W-199)
  {
    R_Date("Poz-149862",29300,350);
    R_Date("ETH-130958",30100,800);
  };
  R_Date("Poz-131676",31800,600);
  R_Date("Poz-129667",33700,600);
  R_Date("Poz-91940",34700,600);
  R_Date("Poz-91895",35500,700);
  R_Date("Poz-91939",35500,700);
  R_Date("Poz-91941",36500,800);
  R_Date("Poz-148301",37300,800);
  R_Date("Poz-148303",38100,900);
  R_Date("Poz-91893",39000,1000);
  R_Date("Poz-148265",39800,1200);
  R_Date("Poz-61113",39900,1100);
  R_Date("Poz-91942",41500,1500);
  R_Date("Poz-148257",41700,1400);
  R_Date("Poz-148256",41900,1400);
  R_Date("Poz-149863",43000,2000);
  R_Date("Poz-148306",43100,1600);
  R_Date("Poz-148304",43100,1900);
  R_Date("Poz-148305",46000,3000);
};
```

OxCal code for sum of distributions of A1 haplogroup Perspektywiczna Cave hyenas

```
Sum("PC hyenas")
{
  R_Date("Poz-129667",33700,600);
  R_Date("Poz-91940",34700,600);
  R_Date("Poz-91895",35500,700);
  R_Date("Poz-91939",35500,700);
  R_Date("Poz-91941",36500,800);
  R_Date("Poz-148301",37300,800);
  R_Date("Poz-148303",38100,900);
  R_Date("Poz-91893",39000,1000);
  R_Date("Poz-148265",39800,1200);
  R_Date("Poz-61113",39900,1100);
  R_Date("Poz-91942",41500,1500);
  R_Date("Poz-148257",41700,1400);
  R_Date("Poz-148256",41900,1400);
  R_Date("Poz-148306",43100,1600);
  R_Date("Poz-148304",43100,1900);
  R_Date("Poz-148305",46000,3000);
};
```

```
};
```

OxCal code for sum of distributions of A2 haplogroup Perspektywiczna Cave hyenas

```
Sum("PC hyenas")
{
  Combine (W-199)
  {
    R_Date("Poz-149862",29300,350);
    R_Date("ETH-130958",30100,800);
  };
  R_Date("Poz-131676",31800,600);
  R_Date("Poz-149863",43000,2000);
};
```

OxCal code for kernel density distributions for all Perspektywiczna Cave hyenas

```
KDE_Model("PC hyenas")
{
  Combine (W-199)
  {
    R_Date("Poz-149862",29300,350);
    R_Date("ETH-130958",30100,800);
  };
  R_Date("Poz-131676",31800,600);
  R_Date("Poz-129667",33700,600);
  R_Date("Poz-91940",34700,600);
  R_Date("Poz-91895",35500,700);
  R_Date("Poz-91939",35500,700);
  R_Date("Poz-91941",36500,800);
  R_Date("Poz-148301",37300,800);
  R_Date("Poz-148303",38100,900);
  R_Date("Poz-91893",39000,1000);
  R_Date("Poz-148265",39800,1200);
  R_Date("Poz-61113",39900,1100);
  R_Date("Poz-91942",41500,1500);
  R_Date("Poz-148257",41700,1400);
  R_Date("Poz-148256",41900,1400);
  R_Date("Poz-149863",43000,2000);
  R_Date("Poz-148306",43100,1600);
  R_Date("Poz-148304",43100,1900);
  R_Date("Poz-148305",46000,3000);
};
```

OxCal code for kernel density distributions for A1 haplogroup Perspektywiczna Cave hyenas

```
KDE_Model("PC hyenas")
{
  R_Date("Poz-129667",33700,600);
  R_Date("Poz-91940",34700,600);
  R_Date("Poz-91895",35500,700);
};
```



```
R_Date("Poz-91939",35500,700);
R_Date("Poz-91941",36500,800);
R_Date("Poz-148301",37300,800);
R_Date("Poz-148303",38100,900);
R_Date("Poz-91893",39000,1000);
R_Date("Poz-148265",39800,1200);
R_Date("Poz-61113",39900,1100);
R_Date("Poz-91942",41500,1500);
R_Date("Poz-148257",41700,1400);
R_Date("Poz-148256",41900,1400);
R_Date("Poz-148306",43100,1600);
R_Date("Poz-148304",43100,1900);
R_Date("Poz-148305",46000,3000);
};
```

OxCal code for kernel density distributions for A2 haplogroup Perspektywiczna Cave hyenas

```
KDE_Model("PC hyenas")
{
  Combine (W-199)
  {
    R_Date("Poz-149862",29300,350);
    R_Date("ETH-130958",30100,800);
  };
  R_Date("Poz-131676",31800,600);
  R_Date("Poz-149863",43000,2000);
};
```